International Journal of Multiphase Flow 158 (2023) 104278

Contents lists available at ScienceDirect

International Journal of Multiphase Flow

journal homepage: www.elsevier.com/locate/ijmulflow

Sensitivity analysis of threshold parameters in slug detection algorithms

F. Webner [a,b], J. Polansky [a,c], S. Knotek [d], S. Schmelter [a,*]

[a] Physikalisch-Technische Bundesanstalt (PTB), Abbestraße 2-12, 10587 Berlin, Germany
[b] German Aerospace Center (DLR), Bunsenstraße 10, 37073 Göttingen, Germany
[c] ESI, Brojova 16, 326 00 Pilsen, Czech Republic
[d] Czech Metrology Institute, Okruzni 31, 638 00 Brno, Czech Republic

ARTICLE INFO

Keywords:
Slug flow
Computational fluid dynamics (CFD)
Slug frequency
Threshold
Sensitivity analysis
Power spectral density (PSD)

ABSTRACT

Slug flow is a common flow pattern in pipelines that is often accompanied by undesirable effects like vibrations, pressure loss, and corrosion. Since these effects correlate with slug frequency, various attempts to predict this parameter by empirical or semi-empirical methods have been undertaken in the past. However, significant mismatches between these predictions can be observed. In this work, different slug frequency calculation methods have been applied to simulation data to investigate the sensitivity of threshold parameters that are often used in slug detection algorithms. The findings reveal that the detection of slugs from liquid holdup data is highly sensitive to these thresholds. Aeration of the liquid phase causes the gas–liquid interface to be less distinct and requires an adaption of the thresholds to the degree of aeration. In contrast, slug detection algorithms based on frequency analysis are robust to small deviations of the liquid level but fail to properly discriminate between slugs and waves. Our investigations show that slug frequency strongly depends on the method chosen for the determination of the liquid level. We propose new approaches that are less susceptible to aeration and approximate the liquid level very close to the authors' human judgment.

1. Introduction

The slug flow pattern is one of the most commonly observed two-phase flow patterns in industrial applications (Pineda-Pérez et al., 2018). For horizontal flow, it is characterized by alternating blocks of aerated liquid (so-called slugs) and gas bubbles flowing above liquid films (Al-Safran, 2009). These liquid slugs can lead to an increased pressure drop, vibrations, as well as increased corrosion and erosion of the pipe (Hill and Wood, 1994; Al-Safran, 2009; Marcano et al., 1998). Hence, they can cause severe problems in industrial operations and lead to large uncertainties in multiphase flow metering (Olbrich et al., 2021a). Because these unfavorable effects strongly correlate to slug frequency (Al-Safran, 2009), this parameter is of special interest.

Due to the inherent unsteady and random behavior of slug flow, it is considered as one of the most complex flow patterns (Marcano et al., 1998), and slug frequency is difficult to predict. Various attempts with empirical and semi-empirical approaches can be found in the literature, see Gregory and Scott (1969), Heywood and Richardson (1979), Hill and Wood (1990), Jepson and Taylor (1993), Al-Safran (2009), Schulkes (2011). However, different slug frequency correlations predict significantly different slug frequencies for the same flow conditions. Even the predicted trends can differ: For the test cases considered in this paper, some correlations predict a slug frequency that decreases monotonically with increasing superficial gas velocity (Schulkes, 2011; Hill and Wood, 1990), whereas others predict opposite trends, either monotonically increasing (Al-Safran, 2009; Jepson and Taylor, 1993) or non-monotonic (Gregory and Scott, 1969; Heywood and Richardson, 1979; Zabaras, 2000). This reveals major difficulties in slug frequency prediction.

The criteria a structure has to meet to be identified as a slug is crucial for the comparison of the predicted or measured slug frequencies of different researchers. Therefore, an idealized slug body was described by Dukler and Hubbard (1975) already in 1975. However, in reality, slugs get aerated remarkably, especially with increasing superficial gas velocity (Andreussi et al., 1993; Gomez et al., 2000), and hence, the slug liquid holdup is reduced significantly (Gregory et al., 1978; Marcano et al., 1998; Abdul-Majeed, 2000). Considering buoyancy effects and the fact that gas entrainment occurs mainly at the slug front at the interface (Dukler and Hubbard, 1975), the liquid holdup is even lower in the upper part of the slug body (Jepson and Taylor, 1993). Hence, the shape of the liquid phase might be significantly distorted compared to the idealized slug model and the gas–liquid interface is less sharp/distinct (Yadigaroglu and Hewitt, 2017). Consequently, different criteria have to be applied to identify slugs.

* Corresponding author.
E-mail address: sonja.schmelter@ptb.de (S. Schmelter).

https://doi.org/10.1016/j.ijmultiphaseflow.2022.104278
Received 12 April 2022; Received in revised form 22 August 2022; Accepted 29 September 2022
Available online 21 October 2022

As established above, these criteria for identifying slugs are crucial for the comparison of slug frequencies determined by different investigations. However, detailed information about the applied criteria are scarce in the literature: Gregory and Scott (1969), Jepson and Taylor (1993), as well as Woods and Hanratty (1999), Woods et al. (2006) identified slugs from pressure pulses but did not mention an exact pressure difference or threshold that had to be surpassed by the slugs to be counted. The latter two (Woods and Hanratty, 1999; Woods et al., 2006) acknowledge the described difficulties and argue that pressure pulses are the preferable method for slug detection because the slug bodies get aerated and it becomes difficult to distinguish waves and slugs by liquid level or liquid holdup at high superficial gas velocities. Marcano et al. (1998), Gokcal et al. (2009), Al-Safran (2009), and Zabaras (2000) utilized capacitance/conductance sensors to determine slug frequencies from liquid holdup, but also without clarifying the exact criteria for a signal to be interpreted as a slug. Moreover, two of these (Al-Safran, 2009; Zabaras, 2000) gathered slug frequency data from the literature, and it is not clear, whether they considered different measurement and calculation methods among their respective data sets. Another instrumentation was utilized by Heywood and Richardson (1979), who measured the liquid holdup by means of the γ-ray absorption method and then performed a power spectral density (PSD) analysis to determine the most dominant frequency, which was considered to be the slug frequency. El-Oun (1990) also utilized γ-rays to determine slug frequency, but the calculation method was not described. In contrast, Hernandez-Perez et al. (2010) declared that a liquid holdup larger than 0.7 is a common criteria for a slug structure and cited Nydal (1991) as a reference. Instead of a fixed liquid holdup threshold, Zhao et al. (2013) as well as Baba et al. (2017) applied a variable threshold, namely the middle between the highest and lowest measured liquid holdup in a time series. More recently, Soedarmo et al. (2019) and Soto-Cortes et al. (2021) developed an automatic threshold selection procedure based on liquid holdup probability density functions for pseudo-slug and slug flow, respectively. They applied a two-threshold approach to identify slug front and tail, which then enabled the calculation of slug length, and hence, slug liquid holdup.

Despite the known difficulties, only little attention has been paid to the exact characteristics of common measurement and calculation methods and their impact on the slug frequency. For high viscosity fluids, Zhao et al. (2013) compared the slug frequencies derived by a thresholding and a PSD method and found good agreement. However, the comparison was limited to low superficial gas velocities, where aeration is low and the shape of the plugs/slugs is more distinct compared to higher superficial gas velocities. This leads to the questions how different slug detection algorithms as well as the parameters used in these methods affect the resulting slug frequency and how thresholding methods compare to frequency analyses by means of PSD at higher superficial gas velocities.

To shed more light on these questions, we simulated horizontal slug flow at seven different superficial gas velocities with the open-source software package OpenFOAM v1812. The numerical simulations provide data for the whole 3D domain. Hence, they give insight into areas that are hardly accessible by experiments. The spatially and temporally resolved liquid volume fraction data enables us to apply and compare different evaluation methods and criteria for the considered test cases. Slug frequency is calculated in two steps: First, the liquid level is estimated from the liquid volume fraction data. Four different approaches are investigated herein. Second, the slug frequency is calculated from the liquid level time series. Here, two fundamentally different methods, namely frequency analysis via PSD and liquid level thresholds, are considered. For the latter one, we conduct a thorough sensitivity analysis of the thresholds that need to be defined for these approaches.

The present work shows how the different calculation methods influence the slug frequency. This clarifies for which cases it is necessary to know the exact criteria of how a slug frequency was determined, and for which part of the plug/slug flow regime the slug frequency is robust and insensitive to the utilized methods. The investigations help to judge slug frequency predictions from the literature that have been determined with different methods and to choose appropriate measurement and calculation methods for slug frequencies in future research.

Table 1
Properties of the fluids used in the numerical simulation.

	Paraflex oil	Nitrogen
Density [kg m^{-3}]	816	10.8
Viscosity [m^2 s^{-1}]	9.6×10^{-6}	1.62×10^{-6}
Surface tension [kg s^{-2}]	0.0286	
Contact angle [°]	72	

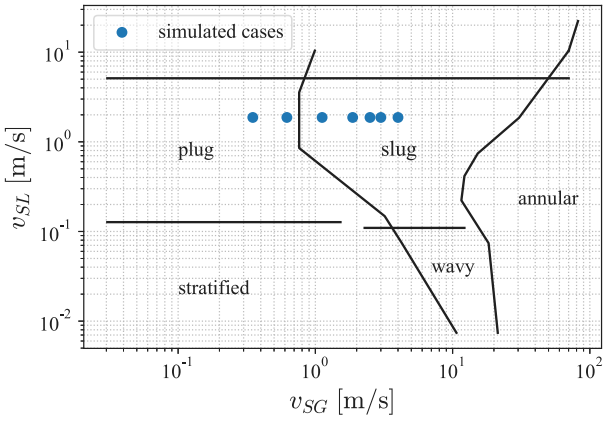

Fig. 1. Simulated test points in the flow pattern map by Mandhane et al. (1974).

2. Simulation methodology

This section describes the general simulation set-up, the utilized schemes, the boundary and initial conditions, as well as a mesh convergence study. We consider the flow of Paraflex oil and nitrogen through a horizontal pipe of inner diameter $D = 0.097$ m and length $L = 305\,D$. The fluid properties prescribed in the numerical simulations are summarized in Table 1. Seven different test cases are considered. All test cases have the same superficial liquid velocity, $v_{sl} = 1.87$ m/s, whereas the superficial gas velocity is different for each case: v_{sg} [m/s] $\in \{0.35, 0.62, 1.12, 1.87, 2.5, 3.0, 4.0\}$. According to the flow pattern map of Mandhane et al. (1974), they all lie within the plug or slug flow regime, where the transition from plug to slug flow occurs at around $v_{sg} = 0.75$ m/s for the considered liquid superficial velocity $v_{sl} = 1.87$ m/s, see Fig. 1.

For the numerical simulation, the open-source software package OpenFOAM v1812 was used. From this package, the two-phase solver `interFoam` was chosen, which is suitable for the transient simulation of two incompressible, isothermal immiscible fluids. It is based on the volume of fluid (VOF) method (Hirt and Nichols, 1981), which is a numerical technique for tracking and locating the interface between two fluids. Since the flow is turbulent, an unsteady Reynolds-averaged Navier–Stokes (URANS) approach was applied. Menter's shear stress transport (SST) turbulence model (Menter, 1993) was employed to close the system of equations.

For the spatial discretization of the pipe geometry, a block-structured mesh was used, see Fig. 2. The refinement level needed for the numerical simulations was determined by means of a grid study. In this study, simulations with a superficial gas velocity of 0.63 m/s were performed for eight different meshes. The results were compared to each other with respect to slug frequency since this is the parameter of interest in this paper. The mesh was refined separately in radial

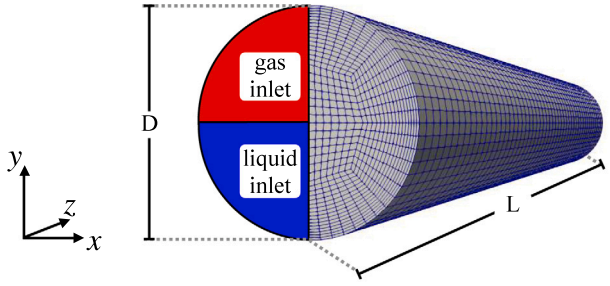

Fig. 2. Illustration of the considered geometry, mesh, and inlet boundary conditions.

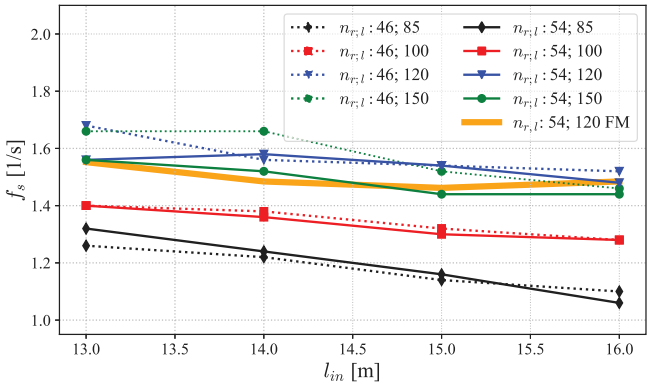

Fig. 3. Comparison of slug frequency over distance to the inlet for different mesh resolutions.

and longitudinal direction. In radial direction, two refinement levels were considered: $n_r = 46/D$ and $n_r = 54/D$, where n_r denotes the number of cells per diameter. In longitudinal direction, four different refinement levels were compared: n_l [1 /m] $\in \{85, 100, 120, 150\}$ with n_l denoting the number of cells per meter in longitudinal direction. To save computational costs, only a pipe length of $L = 165\,D$ instead of the 305 D was considered in the grid study, which is still sufficiently long for the formation of slugs. Furthermore, only half of the pipe geometry was simulated. For this, the computational domain was virtually cut along the vertical symmetry plane in longitudinal direction (yz-plane). A `symmetryPlane` boundary condition was applied to the new face, which was treated like a slip boundary condition (no friction).

Fig. 3 shows the comparison of slug frequency over distance to the inlet for the different mesh resolutions. One can see that the mesh refinement in radial direction has hardly any influence on the resulting slug frequency (compare the solid and dotted lines for each color). The mesh refinement in longitudinal direction, on the other hand, leads to increasing slug frequencies, at least for the first two refinement levels. Nevertheless, grid convergence can be observed for $n_l = 120$ /m and $n_l = 150$ /m. Altogether, it can be concluded that a mesh resolution with $n_r = 46$ cells in radial and $n_l = 120$ cells per meter in longitudinal direction is sufficient.

For four selected meshes (1. $n_r = 46/D, n_l = 85$ /m; 2. $n_r = 46/D, n_l = 100$ /m; 3. $n_r = 54/D, n_l = 85$ /m; and 4. $n_r = 54/D, n_l = 120$ /m), additional simulations for the full geometry (i.e., the whole cylinder) were performed to investigate the effect of simulating only half of the pipe geometry and using symmetry boundary conditions. The investigations showed that, for the coarser meshes, differences in the resulting slug frequencies can be observed. Using the full mesh leads to higher slug frequencies. Hence, it has a similar effect as a grid refinement in longitudinal direction. For the most finest mesh considered in this part of the study ($n_r = 54/D$, $n_l = 120$ /m), these differences become much smaller. In this case, the mean relative error of the slug frequency determined by the half mesh with respect to the full mesh is less than 2.9 %.

Table 2
Spatial discretization schemes used in the numerical simulation.

Scheme	Method
Gradient	Gauss linear
Laplacian	Gauss linear corrected
Divergence	Gauss van Leer/Gauss linear

A brief investigation of required computation time revealed that the shape of the mesh (half or full cylinder) and the resolution in radial direction had a significant impact on computational resources. In contrast, increasing the resolution in longitudinal direction was less demanding. Considering the results of the mesh convergence study and the evaluation of computational resources, a mesh of half-cylindrical shape with a resolution of $n_r = 46/D$ and $n_l = 14/D \approx 144$ /m was used for the numerical simulations. The final calculations were run on a high performance cluster using 24 processors for each simulation. Depending on the prescribed superficial gas velocities, a simulation of 70 s took between one and four weeks (higher superficial gas velocities were computationally more demanding).

For the time discretization, the implicit Euler scheme was used. The time step size was adjusted automatically by limiting the Courant number to 0.5. The total simulation time was 70 s. The schemes used for the spatial discretization are summarized in Table 2. Regarding initial conditions, at the start of the simulation, the pipe contains no liquid and an initial velocity of 0 m/s is defined. On the pipe walls, no-slip boundary conditions are applied. The inlet cross section was bisected horizontally as shown in Fig. 2. The gas enters the pipe through the upper part, the liquid through the lower part of the inlet. To enhance slug initiation, the inlet perturbation method by Schmelter et al. (2021a) is used. In this approach, the secondary velocity components (parallel to the inlet face) are changed over time. They are chosen randomly in direction and amplitude, but only up to 20 % of the main component's amplitude. Since only the secondary velocity components are disturbed, the total volume flux is not influenced. This approach enhances the formation of slugs in the pipe, which is beneficial for computational costs because the length of the domain can be reduced. Furthermore, in Schmelter et al. (2021a) it is shown that the mean slug frequency at downstream locations converges for different perturbation amplitudes. Hence, it can be concluded that the inlet perturbations do not affect the slug frequency in developed slug flow.

3. Extraction of liquid level time series from simulation results

To calculate the slug frequency f_s, the liquid level is analyzed. According to Andritsos and Hanratty (1987), it is defined as the vertical position of the gas–liquid interface relative to the inner pipe diameter in the vertical centerline of the pipe cross section. This means that "liquid level" refers to the dimensionless liquid level $h_l = h_d/D$, where h_d is the dimensioned liquid level, i.e., the height of the liquid–gas interface in the middle of the pipe. However, determining the liquid level is not trivial. In this section, we describe several methods to approximate the liquid level.

3.1. Approximation of liquid level based on area-average of liquid volume fraction

The liquid holdup H_l at a fixed longitudinal position z in the pipe is calculated as the area-average of the liquid volume fraction $\alpha(x, y, z, t)$ for all time points t as

$$H_l(z,t) = \frac{1}{A}\int_A \alpha(\cdot,\cdot,z,t)\,dA = \frac{1}{A}\int_{-D/2}^{D/2}\int_0^D \alpha(x,y,z,t)\,dx\,dy. \quad (1)$$

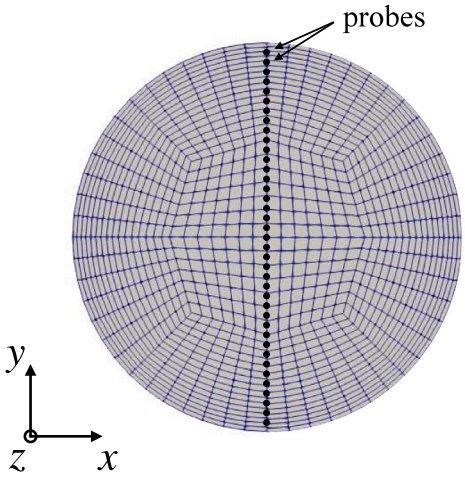

Fig. 4. Illustration of the probes used for the calculation of the liquid level h_l^{line}.

Here, A denotes the cross-sectional area of the pipe: $A = \pi(D/2)^2$, where D is the inner diameter of the pipe.

Under the assumption of a plain, horizontal interface between liquid and gas, the liquid holdup H_l is equivalent to the area of a circular segment and can be used to approximate the liquid level h_l^{area} by solving the following equation iteratively:

$$H_l(z,t) = r^2 \arccos\left(1 - \frac{h_l^{\text{area}}(z,t)}{r}\right) - (r - h_l^{\text{area}}(z,t))\sqrt{r^2 - (h_l^{\text{area}}(z,t) - r)^2}, \quad (2)$$

where $r = D/2$ is the radius of the cross section. The liquid holdup is a parameter that is often used in measurements to determine slug frequencies (e.g., in Marcano et al. (1998), Heywood and Richardson (1979), Gokcal et al. (2009), Zhao et al. (2013), Baba et al. (2017)). By means of Eq. (2) such measurements of H_l can easily be converted into a corresponding liquid level h_l^{area}. The conversion into h_l^{area} allows a better comparison with the liquid levels introduced in the following.

3.2. Approximation of liquid level based on line-average of liquid volume fraction

Instead of averaging the liquid volume fraction over the whole cross-sectional area A, in the following approach, it is only averaged over the vertical centerline of the pipe cross section:

$$h_l^{\text{line}}(z,t) = \frac{1}{D}\int_0^D \alpha(x=0,y,z,t)dy. \quad (3)$$

To calculate h_l^{line} numerically, $N = 39$ probes are located equidistantly with a distance of $D/(N+1) = D/40$ to each other and to the walls, see Fig. 4.

The liquid level is then approximated by:

$$h_l^{\text{line}}(z,t) = \frac{1}{N+1}\left(1.5\left(\alpha(0,y_1,z,t)+\alpha(0,y_N,z,t)\right) + \sum_{i=2}^{N-1}\alpha(0,y_i,z,t)\right), \quad (4)$$

where y_1 and y_N are the outmost probe locations. These probes represent the distance between the probe and the wall of $D/(N+1)$ plus half of the distance to the next probe of $D/(2(N+1))$. Thus, they cover 1.5 times more distance than the inner probes at locations y_i, $i = 2,\dots,N-1$.

In a separated flow with a level interface, this would yield the liquid level with a tolerance of the distance between the probes of $D/(N+1)$. However, due to aeration of the liquid phase or liquid droplets in the gas phase, the liquid level determined by this method can be lower or higher than the actual liquid level. Bubbles and droplets that intersect with one of the N probes have a larger impact on the liquid level determined by this method compared to the previous method based on the liquid holdup.

To account for bubbles included in the liquid phase, which are typical for slug flow, the following correction algorithm is proposed. In a first iteration, h_l^{line} is calculated. In a second step, an auxiliary liquid volume fraction α^{impr} is calculated by setting all liquid volume fraction values of probes located below h_l^{line} to one. Then, the average of the auxiliary liquid volume fraction is calculated. Altogether, h_l^{impr} is determined similar to (4) using α^{impr} instead of α:

$$h_l^{\text{impr}}(z,t) = \frac{1}{N+1}\left(1.5\left(\alpha^{\text{impr}}(0,y_1,z,t)+\alpha^{\text{impr}}(0,y_N,z,t)\right) + \sum_{i=2}^{N-1}\alpha^{\text{impr}}(0,y_i,z,t)\right), \quad (5)$$

where $\alpha^{\text{impr}}(y_i,z,t)$, $i = 1,\dots,N$, is given by

$$\alpha^{\text{impr}}(y_i,z,t) = \begin{cases} 1 & y_i \le h_l^{\text{line}}(z,t). \\ \alpha(0,y_i,z,t) & \text{otherwise.} \end{cases} \quad (6)$$

In a truly separated flow, no bubbles occur and all probes below h_l^{line} automatically attain the value of one. In this case, $h_l^{\text{impr}} = h_l^{\text{line}}$. In case of slug flow with a lot of aeration, on the other hand, $h_l^{\text{impr}} > h_l^{\text{line}}$.

Fig. 5 shows three plots of the liquid volume fraction over time at the N probes for three different superficial gas velocities: v_{sg} [m/s] $\in \{0.35, 1.87, 4.0\}$. Each dot represents the liquid volume fraction (α) of the respective time and y-position. The higher the liquid volume fraction, the darker the dot. A black dot represents the liquid phase ($\alpha = 1$) and a white one the gas phase ($\alpha = 0$). Furthermore, the approximations of the liquid level determined by the three different methods, h_l^{area}, h_l^{line}, and h_l^{impr}, are shown. The time intervals were chosen to demonstrate the representative characteristics of each method. In an ideally separated flow, the interface and, therefore, the liquid level could be determined unambiguously at the point of transition between alpha values of zero and one. This is nearly the case for $v_{sg} = 0.35$ m/s, where the phases are clearly separated. Hence, all three methods align well. For $v_{sg} = 1.87$ m/s, on the other hand, significant differences between the liquid level approximations can be observed at 14.6 s, where a gas bubble is enclosed in the liquid phase. (Note that the shape of the bubble is distorted and squashed by this visualization). In this case, h_l^{line} and h_l^{area} both underestimate the liquid level, whereas h_l^{impr} is able to predict it correctly. At around 14.52 s, droplets in the air lead to a slight overestimation of the liquid level by h_l^{line}. This overestimation is further increased by h_l^{impr}. For $v_{sg} = 4.0$ m/s, the aeration increases and the differences between the averaging methods compared to h_l^{impr} become more apparent: The averaging methods never capture the actual height of the wave structure, whereas h_l^{impr} reproduces the shape of the wave significantly better. At around 30.69 s, h_l^{impr} exhibits a downward peak because the aeration/bubble is partly above h_l^{line}. This illustrates how the aeration below h_l^{line} is added to h_l^{line} to yield h_l^{impr}.

3.3. Approximation of liquid level based on binary methods

The idea of this approach is to convert the continuous liquid volume fraction field α into a field of binary values (either 0 or 1) by means of a threshold θ_{bin}. If $\alpha > \theta_{\text{bin}}$, the fluid is counted as liquid. Otherwise, it is considered as gas. The liquid level h_l^{bin} at time t is then defined as the highest y-position occupied by liquid:

$$h_l^{\text{bin}}(z,t) = \frac{1}{D}\max\{y \in [0,D] | \alpha(x=0,y,z,t) > \theta_{\text{bin}}\}. \quad (7)$$

Using the previously defined probes at locations y_i, $i = 1,\dots,N$, it can be approximated as follows:

$$h_l^{\text{bin}}(z,t) \approx \frac{1}{D}\max\{y_i, i = 1,\dots,N | \alpha(x=0,y=y_i,z,t) > \theta_{\text{bin}}\}. \quad (8)$$

Fig. 6 illustrates this method for two different thresholds $\theta_{\text{bin}} = 0.5$ and $\theta_{\text{bin}} = 0.8$. Similarly to Fig. 5, three plots are shown for v_{sg} =

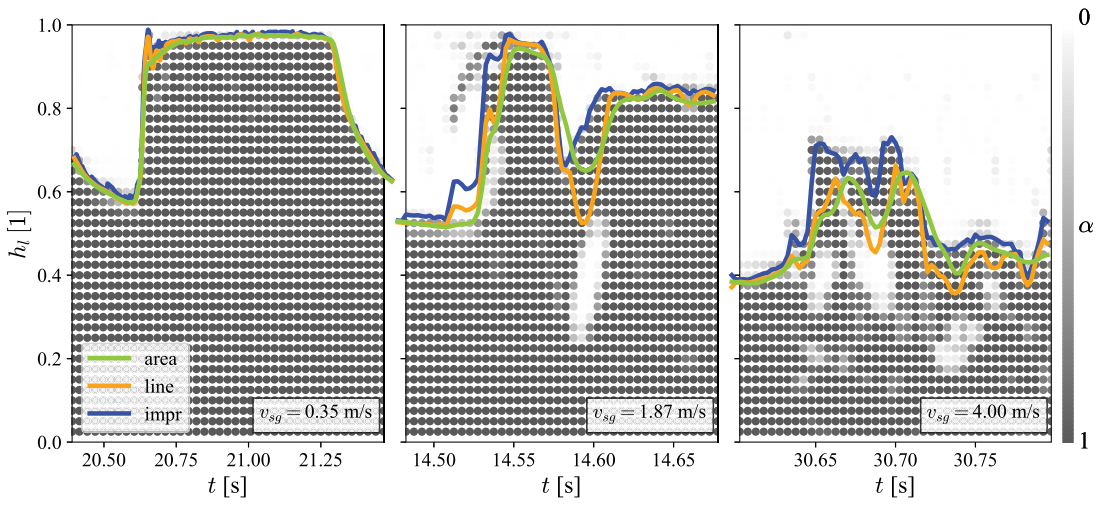

Fig. 5. Approximations of the liquid level by h_l^{area}, h_l^{impr}, and h_l^{line} plotted in the liquid volume fraction field for $v_{sg} = 0.35$ m/s (left), 1.87 m/s (middle), and 4.0 m/s (right).

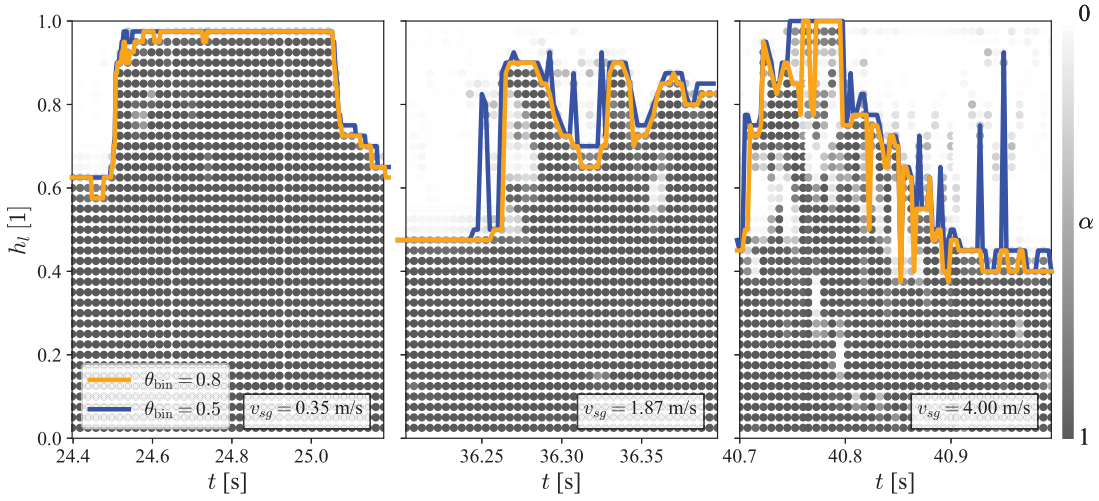

Fig. 6. Approximation of the liquid level by h_l^{bin} for two different thresholds θ_{bin}= 0.5 and θ_{bin}= 0.8 plotted in the liquid volume fraction field for $v_{sg} = 0.35$ m/s (left), 1.87 m/s (middle), and 4.0 m/s (right).

0.35 m/s, 1.87 m/s, and 4.0 m/s, respectively, where the time interval is again chosen to demonstrate the characteristics of the compared methods. For low aeration with a clear interface (v_{sg} = 0.35 m/s), the different thresholds θ_{bin} = 0.5 and θ_{bin} = 0.8 yield nearly the same results. However, when the superficial gas velocity is increased, individual droplets cause the h_l^{bin} to jump for θ_{bin} = 0.5. Because the droplets usually have a low liquid volume fraction value, the graph for θ_{bin} = 0.8 remains smooth and reproduces the shape of the liquid structure better. When the superficial gas velocity is increased further, as shown in the plot with v_{sg} = 4 m/s, the number of spikes caused by individual droplets increases for θ_{bin} = 0.5. In contrast, the graph for θ_{bin} = 0.8 exhibits downward spikes because of aeration. However, while an individual droplet in the gas phase is sufficient to cause an upward spike, an individual bubble in the liquid phase cannot cause a downward spike (because of the maximum used in the definition of h_l^{bin}). Therefore, the downward spikes that are typical for high thresholds θ_{bin} occur more rarely and are less pronounced.

4. Calculation of slug frequency from liquid level time series

The slug frequency is the number of slugs that passes a specific point along the pipeline over a certain period of time (Al-Safran, 2009). In this work, we considered a time interval of 50 s (the initial 20 s of the simulation were omitted) and evaluated the slug frequency at position $z = 300\,D$ downstream from the inlet. For the detection of slugs from the liquid level time series, two different approaches are used. The first one is based on defining thresholds for slug detection, the second one uses frequency analysis.

4.1. Thresholds for slug detection

Soto-Cortes et al. (2021) and Soedarmo et al. (2019) applied a two threshold method to identify the slug front and slug tail, respectively. This allows to calculate the slug length and suppresses double counting of the same slug structure. For the present investigation, a similar methodology with two thresholds is applied. However, a simpler approach is used. This could be done because the thresholds discussed herein are solely evaluated to determine slug frequency but not slug length. When the liquid level exceeds the upper threshold θ_{up} a slug is counted. The lower threshold θ_{low} makes sure that small fluctuations of the liquid level do not lead to double counting of slugs.

Choice of upper threshold. The upper threshold θ_{up} defines the required minimum liquid level of a structure to be identified as a slug. A typical characteristic of slugs is that the liquid phase occupies the whole cross section. Thus, for ideal slugs, the liquid level should increase to one. Hence, for the methods that compensate aeration, like h_l^{bin} and h_l^{impr},

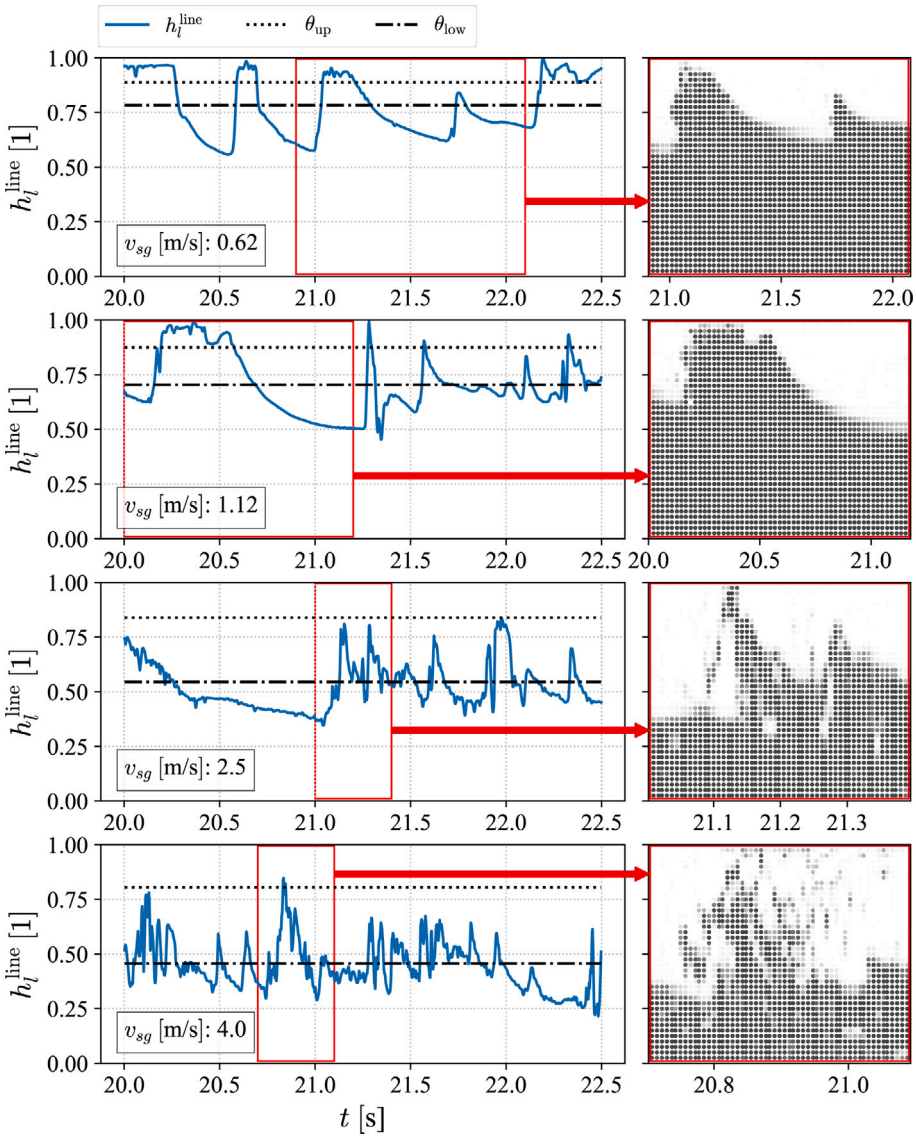

Fig. 7. Visualization of θ_{up} and θ_{low} for exemplary cases.

an upper threshold θ_{up}=0.95 (i.e., a value close to 1) is chosen. On the other hand, a much lower value for θ_{up} is needed for methods that do not take aeration into account. To determine an appropriate value for θ_{up} for these methods, the aeration of the slugs is estimated by means of slug holdup prediction methods from the literature. A review of several methods is presented in Appendix A. If not stated otherwise, we use the slug holdup prediction by Gomez et al. (2000). Eq. (2) is utilized to convert the liquid holdup of the slugs into a corresponding liquid level. As mentioned early on, not all researchers describe the exact method how they calculated the slug frequencies. However, using liquid level or liquid holdup thresholds as explained here appears to be a popular method, see Hernandez-Perez et al. (2010), Baba et al. (2017), Zhao et al. (2013), Fabre et al. (1995).

Choice of lower threshold. The lower threshold θ_{low} can be understood as a threshold to identify the tail of a slug body. Bubbles or an uneven liquid surface may cause the liquid level of a slug body to fluctuate and cross θ_{up} several times. The lower threshold assures that these fluctuations are still accounted to the same slug body until the liquid level falls below θ_{low}. It is chosen as the value of the average liquid level. As shown below in Section 5.1, this value is a good choice for slug detection.

Fig. 7 illustrates the choice of upper and lower thresholds for h_l^{line} for four different cases. For each case, a slug structure is marked with a red rectangle, and a plot of the liquid volume fraction of the corresponding time interval is shown on the right. This illustrates the fraction of liquid and gas inside the slug structure. For the case with a superficial gas velocity of 0.62 m/s, four slug structures and one wave at around 21.75 s can be visually identified. If the liquid level of a slug structure fluctuates around θ_{up}, e.g., at 22.4 s, then θ_{low} prevents double counting of slugs until the liquid level falls below θ_{low}. The liquid volume fraction plot on the right hand side shows a slug structure and the wave. It also shows that the fluid phases are well separated.

For the 2.5 m/s case, the liquid level does not exceed θ_{up} between 21.0 s and 21.5 s. However, the liquid volume fraction plot reveals that the liquid phase is aerated and reaches the top of the pipe. This demonstrates how aeration affects the calculated liquid level and why θ_{up} has to be adapted to the superficial gas velocity or slug holdup. However, each slug is unique and may have a different shape and level of aeration. Therefore, a certain θ_{up} might be too high to detect all slugs, but too low to also count waves as slugs at the same time.

Comparing the liquid volume fraction plots on the right, one observes how aeration increases with higher superficial gas velocities. In the plots of the liquid level time series (left picture), on the other hand,

Table 3
Parameters used for the calculation of `pwelch`.

Parameter	Value
Sampling frequency	400
Segment length	600
Overlap	0
Number of DFT points	6000

a change from relatively smooth curves to curves with a lot of peaks and oscillations can be observed, indicating the transition from plug to slug flow at a superficial gas velocity of around 1.12 m/s. This value is in a similar range as the value predicted by the flow pattern map of Mandhane et al. (1974), see Fig. 1.

4.2. Frequency analysis

Another approach to determine slug frequency from liquid level time series is frequency analysis. It is, for example, applied in Hernandez-Perez et al. (2010), Knotek et al. (2016), Schmelter et al. (2021a). One advantage of frequency analysis is that no thresholds need to be chosen in advance. Furthermore, frequency analysis methods (like a Fourier transform) are easy to apply. On the other hand, the most dominant frequencies determined by these methods are not necessarily the frequencies of the slugs, but only reflect the dynamics of the interface between the different phases (Schmelter et al., 2021a; Knotek et al., 2021).

In this paper, Welch's PSD estimate (function `pwelch` in Matlab) was applied to the liquid level time series at position $z = 300\,D$. The function `pwelch` calculates the one-sided PSD estimate using Welch's segment averaging estimator, see The MathWorks, Inc. (2019) for details. Due to additional smoothing, it is more robust than a pure Fourier transform. Table 3 summarizes the parameters used for the computation of `pwelch`. In the simulation, data were saved every 0.0025 s leading to a sampling frequency of 400 Hz. Hence, the segment length of the filter corresponds to a time interval of 1.5 s. The number of points used in the discrete Fourier transform (DFT) corresponds to a time interval of 15 s.

5. Results and discussion

In the following, we discuss the sensitivity of slug frequency to different slug detection algorithms as well as to the parameters used in these methods. In Section 5.1, the influence of thresholds on the slug frequency is investigated. Then, in Section 5.2, the effect of the prediction of the liquid holdup in slugs is discussed. Finally, a comparison of the different methods is presented in Section 5.3.

5.1. Sensitivity of slug frequency to thresholds

As established above, a lot of slug detection algorithms use thresholds to decide whether a structure is counted as slug or not. In the following, the sensitivity of the resulting slug frequency with respect to these thresholds is presented.

In Fig. 8, the slug frequency determined from h_l^{area} is plotted against θ_{up}. The solid lines represent the slug frequencies determined with θ_{low} equal to the average liquid level, whereas the dotted lines show the slug frequency determined with θ_{low} equal to θ_{up}, which is equivalent to not utilizing a lower threshold. The circles on each solid curve mark the thresholds based on the slug holdup estimation by Gomez et al. (2000). This estimation is described in detail in Appendix A. If a lower threshold θ_{bin} is used, one observes hardly any sensitivity to θ_{up} for the cases in the plug flow regime, i.e., superficial gas velocities of 0.35 m/s and 0.62 m/s. The corresponding lines are close to constant for $\theta_{\text{up}} < 0.95$. On the other hand, for cases with higher superficial gas velocity, the resulting slug frequency depends strongly on the choice of θ_{up}. Thus, the choice of θ_{up} is crucial for the determination of the slug frequency. Because θ_{up} has to be larger than θ_{low} and θ_{low} is different for each case, the solid curves for each case are defined on different intervals. The comparison of the dotted lines with the corresponding solid lines exhibits the effect of utilizing a lower threshold. The lower threshold always reduces the determined slug frequency, which is particularly significant for low superficial gas velocities. This is because the lower threshold prevents fluctuations of the liquid level of a slug body to be counted as slugs, see top picture in Fig. 7. Hence, a lower threshold is necessary to distinguish between several slug structures on one hand and fluctuations of the liquid level within one slug structure on the other hand. For h_l^{line} and h_l^{impr} (not shown here), similar observations can be made as for h_l^{area}. For h_l^{impr}, the key difference is that all slug frequencies are slightly increased, and, therefore, all curves are shifted to the right.

In summary, the slug frequency is highly sensitive to θ_{up}. Furthermore, θ_{low} is efficient to avoid the double counting of slugs due to fluctuations in the liquid level within one slug structure.

Fig. 9 shows the slug frequency determined from h_l^{area} plotted against θ_{low} to visualize the sensitivity of the slug frequency to θ_{low}. The plotted intervals are not identical for each curve because θ_{low} has to be lower than θ_{up}, and all curves are evaluated for different values of θ_{up} corresponding to the slug holdup predicted by Gomez et al. (2000). The average liquid level of each case, which has been chosen as "default value" for the lower threshold in this paper, is marked with a dot on each curve. The chosen thresholds generally lie within an interval of almost constant slug frequency, especially for cases with either high or low superficial gas velocity. The largest influence of θ_{low} on the resulting slug frequency is observed for cases with medium superficial gas velocities v_{sg} [m/s] $\in \{1.12, 1.87, 2.5\}$. However, the influence is still small compared to θ_{up}. This shows that small deviations of the chosen θ_{low} have a low impact on the determined slug frequency. Again, similar trends are observed for h_l^{line} and h_l^{impr}, where h_l^{impr} generally yields higher slug frequencies.

Table 4 shows how the slug frequency changes when the thresholds θ_{low} and θ_{up} are increased or decreased by 0.05. θ_{low} has the largest impact on the case with a superficial gas velocity of 1.12 m/s, where the slug frequency is reduced by 17.9 %, when θ_{low} is reduced. In average decreasing or increasing θ_{low} by 0.05, changes the slug frequency by −5.2 % and +3.9 %, respectively.

In contrast, a deviation of the chosen θ_{up} by 0.05 increases or decreases the slug frequency by at least 33.9 % for cases with superficial gas velocities of 1.12 m/s or higher. In average, decreasing θ_{up} by 0.05 increases the slug frequency by 92.1 %, whereas reducing θ_{up} reduces the slug frequency by 46.3 %. This shows that the choice of θ_{up} has a large impact on the resulting slug frequency, at least for the cases in the slug flow regime (i.e., superficial gas velocity of 1.12 m/s and higher), whereas the slug frequency is much less sensitive to θ_{low}.

Fig. 10 shows the sensitivity of the slug frequency with respect to the binary threshold θ_{bin} used in h_l^{bin}. As a reminder, the slug frequencies from h_l^{bin} are all calculated with an upper threshold $\theta_{\text{up}} = 0.95$ since aeration is taken into account by h_l^{bin}. For each case, the slug frequency exhibits a decreasing trend for increasing θ_{bin}. Setting $\theta_{\text{bin}} = 0.5$ seems intuitive to separate the gas from the liquid phase. However, as previously shown in Fig. 6, droplets in the gas phase may cause significant fluctuations of h_l^{bin} for low values of θ_{bin}. For the cases with relatively low superficial gas velocities (v_{sg} [m/s] $\in \{0.35, 0.62, 1.12\}$), slug frequency is almost equal for $\theta_{\text{bin}} = 0.5$ and $\theta_{\text{bin}} = 0.8$. Most cases in the slug flow regime show a (light) dependency on θ_{bin} in this range, presumably because droplets are less miscounted as slugs for higher thresholds θ_{bin}. Therefore, a threshold $\theta_{\text{bin}} = 0.8$ is chosen, and the corresponding slug frequencies are marked with dots in the figure.

In Fig. 10, one can also observe that the slug frequency decreases with increasing superficial gas velocity and that the f_s-over-θ_{bin} curves do not cross each other. Only the 1.12 m/s case, which is close to the

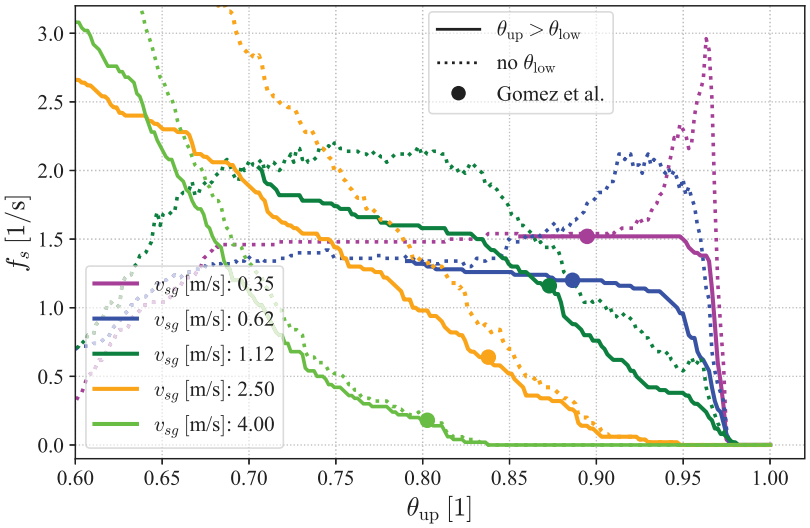

Fig. 8. Slug frequency f_s over upper threshold θ_{up} for five selected test cases with and without utilization of lower threshold θ_{low}. The circles mark the chosen θ_{up} for these cases and the respective slug frequencies.

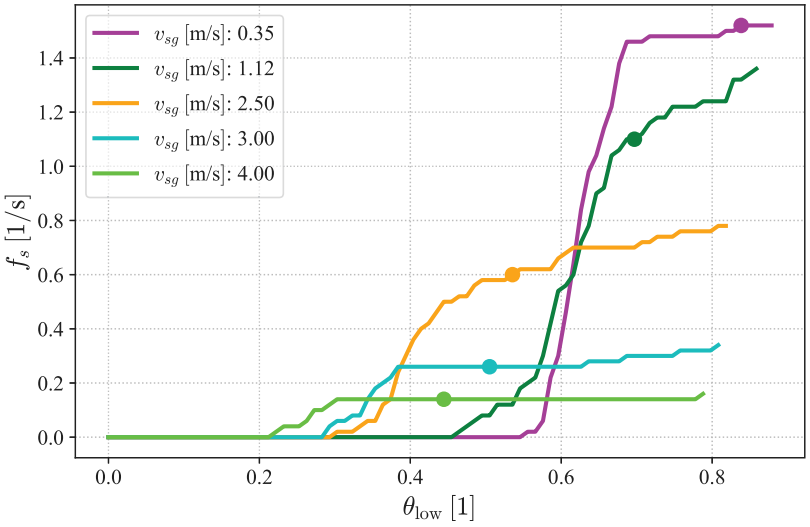

Fig. 9. Slug frequency f_s over lower threshold θ_{low} for five selected cases. The circles mark the chosen θ_{low} for these cases and their respective slug frequencies.

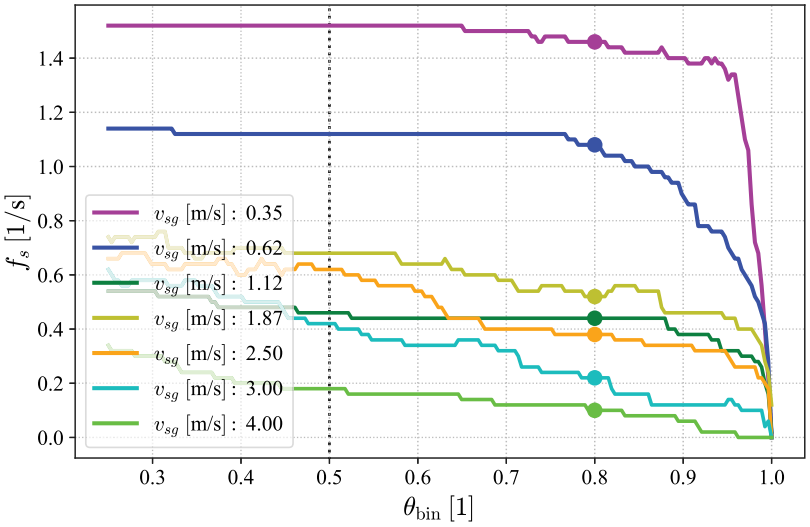

Fig. 10. Slug frequency f_s over binary threshold θ_{bin} for all cases. The circles mark the chosen θ_{bin} for each case and the respective slug frequencies.

Table 4
Respective impact of changing θ_{low} and θ_{up} by 0.05 on slug frequency.

v_{sg}	f_s	$f_s(\theta_{low}) - f_s(\theta_{low} \pm 0.05)$				$f_s(\theta_{up}) - f_s(\theta_{up} \pm 0.05)$			
		−0.05		+0.05		−0.05		+0.05	
[m/s]	[1/s]	[1/s]	[%]	[1/s]	[%]	[1/s]	[%]	[1/s]	[%]
0.35	1.52	−0.04	−2.6	+0.02	+1.3	+0.02	+1.3	−0.0	−0.0
0.62	1.20	−0.02	−1.7	+0.06	+5.0	+0.06	+5.0	−0.08	−6.7
1.12	1.12	−0.20	−17.9	+0.10	+8.9	+0.38	+33.9	−0.66	−56.9
1.87	0.76	−0.06	−7.9	+0.04	+5.3	+0.42	+55.3	−0.28	−36.8
2.50	0.62	−0.04	−6.5	+0.04	+6.5	+0.48	+77.4	−0.4	−62.5
3.00	0.26	−0.00	−0.0	+0.0	+0.0	+0.78	+300.0	−0.16	−61.5
4.00	0.14	−0.00	−0.0	+0.0	+0.0	+0.24	+171.4	−0.14	−100.0
Average:		−0.05	−5.2	+0.04	+3.9	+0.34	+92.1	−0.25	−46.3

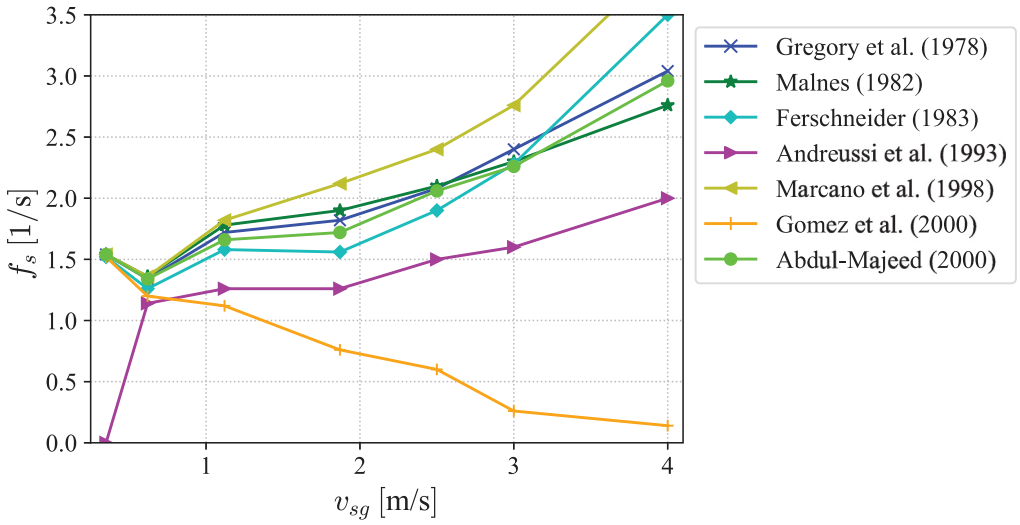

Fig. 11. Slug frequencies determined from h_l^{area} with different slug holdup estimations.

plug-to-slug flow transition as observed in Fig. 7, is an exception to both observations.

For superficial gas velocities of 2.5 m/s or larger, Fig. 8 revealed that the slug frequency drops to 0 /s for $\theta_{up} = 0.95$. This indicates that h_l^{area} never exceeds values of 0.95 for these cases. In contrast, Fig. 10 shows slug frequencies greater than 0 for $\theta_{bin} = 0.95$ for all superficial gas velocities. This shows that the liquid phase reaches almost the top of the pipe, but aeration reduces the liquid level predicted by h_l^{area}.

5.2. Sensitivity of slug frequency to liquid holdup prediction

As aforementioned, an estimation of the slug holdup is required to calculate the slug frequency from h_l^{area} and h_l^{line}, and we exemplarily utilized the prediction by Gomez et al. (2000) in the previously presented investigations. However, a variety of different slug holdup estimations can be found in the literature. Some of them are briefly presented in Appendix A, namely Gregory et al. (1978), Malnes (1982), Ferschneider (1983), Andreussi et al. (1993), Marcano et al. (1998), Gomez et al. (2000), and Abdul-Majeed (2000). Note that, the selection of methods is based on the two review papers by Pereyra et al. (2012) and Ibarra et al. (2019). To investigate how the choice of the slug holdup correlation affects the resulting slug frequency, we calculated the slug frequency from h_l^{area} multiple times, each time with a different θ_{up} according to each slug holdup correlation. Fig. 11 shows the seven different predictions of the slug frequency for the seven different slug holdup correlations spanning a large range of slug frequencies.

Andreussi et al. (1993) predict a slug liquid holdup of 0.998 for $v_{sg} = 0.35$ m/s (see Appendix A). A value of this magnitude can only be achieved by ideal plugs/slugs so that it results in a slug frequency of 0 /s in the simulation data. All other slug liquid holdup predictions result in a similar slug frequency of about 1.5 (slugs) per second at $v_{sg} = 0.35$ m/s. For $v_{sg} = 0.62$ m/s, the slug frequency decreases to values between about 1 and 1.35 (slugs) per second for all slug holdup prediction methods. If the superficial gas velocity is further increased, however, the slug frequencies do not show the same trend anymore, but diverge and, hence, span a remarkable range. This is in line with the observations made in Fig. 8 that the slug frequency is less sensitive in the plug flow region, but aeration and lower slug liquid holdups make slug frequency more sensitive to the upper threshold for higher superficial gas velocities in the slug flow region. This is particularly troublesome, when the upper threshold is based on other sensitive quantities like the slug liquid holdup.

Summed up, Fig. 11 reaffirms that the thresholding methods are highly sensitive to the chosen upper threshold (that is based on slug liquid holdup estimations), especially in the slug flow region. This means that two slug frequency predictions based on the same data set can differ completely if thresholds based on different holdup estimations are chosen.

5.3. Comparison of different slug frequency calculation methods

In previous sections, four different approximations of the liquid level (Sections 3.1–3.3) as well as two methods to calculate the slug frequency from the liquid level were described (Sections 4.1–4.2). Therefore, eight combinations of liquid level approximations and slug detection algorithms are possible. In Fig. 12, these eight slug frequency predictions are plotted over the superficial gas velocity. The four liquid level approximations (h_l^{bin}, h_l^{impr}, h_l^{area}, h_l^{line}) are discerned by different colors, while the slug detection algorithms (thresholding and PSD) are plotted in solid and dashed lines, respectively. For the thresholding

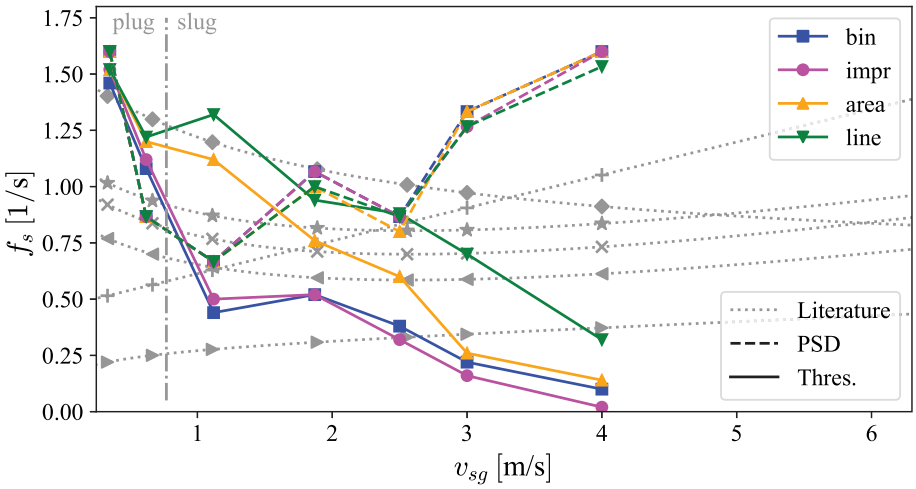

Fig. 12. Comparison of evaluation methods with slug frequency prediction methods from literature.

algorithms utilizing h_l^{area} and h_l^{line}, a variable upper threshold based on the liquid holdup by Gomez et al. (2000) was applied, as described earlier in Section 4.1. Conversely, a fixed upper threshold of 0.95 was applied for h_l^{bin} and h_l^{area} because those two liquid level approximations compensate for aeration.

Furthermore, several slug frequency predictions from the literature (Al-Safran, 2009; Gregory and Scott, 1969; Heywood and Richardson, 1979; Jepson and Taylor, 1993; Schulkes, 2011; Zabaras, 2000) are plotted by gray dotted lines with markers. For more details about these prediction methods, the reader is referred to Appendix B, where the markers are assigned to their designated references.

Fig. 12 allows several observations: first, all eight determined slug frequencies exhibit a decreasing trend over superficial gas velocity and align well with each other in the plug flow regime, where aeration is low and high liquid levels are obtained over a sustained period of time. In contrast, the slug frequencies determined by PSD and thresholding behave differently in the slug flow regime, and the differences increase with superficial gas velocity. At superficial gas velocities between v_{sg} = 2.5 m/s and v_{sg} = 4 m/s, two groups can be recognized: The slug frequencies determined by the PSD show a generally increasing trend of slug frequency over superficial gas velocity, whereas the thresholding method results in a falling trend.

This first observation partly matches with the results reported by Zhao et al. (2013). An important difference is that Zhao et al. (2013) reported a good match between PSD and thresholding up to superficial gas velocities of 2 m/s, whereas we observed large discrepancies between the methods already for superficial gas velocities of 1.12 m/s. However, Zhao et al. (2013) performed their comparison for superficial liquid velocities of 0.1 m/s, which, according to the flow pattern map shown in Fig. 1, shifts the plug-to-slug flow transition to higher superficial gas velocities. Hence, their results are in good agreement with the observations made in this study.

Second, the four PSD curves match each other closely, which implies that the considered methods of liquid level approximation is less relevant for the slug frequency and that the simplest approximation may suffice in this case. In contrast, the thresholding method obtains a wide spread of slug frequencies for the different liquid level approximations.

And third, among the thresholding methods, the slug frequencies based on h_l^{bin} and h_l^{impr} match closely, which are the two approximations that compensate for aeration and aim to detect the highest point of the liquid phase. In contrast, h_l^{area} and h_l^{line}, which are based on averages of the liquid volume fraction, both yield different results compared to the other methods. These deviations can be explained by the inconsistent predictions of the liquid holdup from the literature, see Fig. 11.

The thresholding methods aim to identify actual slug structures, while the PSD is only able to identify dominant structures, but it is not clear whether these dominant structures are indeed slugs or only waves. It is a well-known drawback of methods based on frequency analysis that they cannot clearly distinguish between waves and slugs (Schmelter et al., 2020; Knotek et al., 2021; Schmelter et al., 2021b). The slug frequency based on thresholding of h_l^{bin} is not expected to underestimate the slug frequency, because a single probe located at $y \geq 0.95\,D$ measuring a liquid volume fraction of ≥ 0.8 (see Section 3.3) is sufficient to trigger a slug being counted. Therefore, we assume that the thresholding methods for h_l^{area} and h_l^{line}, and especially the PSD method (for all four liquid level approximations) overestimate the slug frequency in the slug flow regime. This shows that the height of the liquid structure cannot reliably be determined either by PSD or liquid holdup. Hence, the methods that aim to detect the top of the liquid phase, i.e., h_l^{bin} and h_l^{impr}, are less susceptible to aeration and perform best.

Another observation in Fig. 12 is made by comparing the calculated slug frequencies with predictions from literature. Among the predicted slug frequencies, the values and trends of slug frequencies differ remarkably. Monotonic increasing, monotonic decreasing, as well as non-monotonic slug frequency predictions can be found in the literature. For example, the prediction by Heywood and Richardson (1979) exhibits a non-monotonic trend and is based on slug frequencies derived by PSD, which is in line with our results. The slug frequency predictions also reveal a high uncertainty throughout the shown interval, where slug frequencies range from 0.25 to 1.25 slugs per second, for instance at the slug-to-plug flow transition. For medium superficial gas velocities (0.65 m/s $\leq v_{sg} \leq$ 2.5 m/s), our results lie within the range of predicted slug frequencies. Of note, many slug frequency predictions are based on mixed data published or provided by several individual research teams. One can readily see that the average of our eight calculated slug frequencies would fit in the predictions very well.

6. Conclusions

Difficulties in slug frequency prediction have been observed in the literature. Possible reasons are the random and unsteady nature of slug flow, the large variety of parameters that influence slug frequency as well as inaccurate liquid holdup measurements, e.g., by tomography (Olbrich et al., 2021b). However, also the approaches used to determine the holdup or liquid level in the pipe as well as the methods used to calculate the slug frequency have an influence on the resulting slug frequency.

To assure that the applied method is feasible to determine the slug frequency, researchers often verify their approach by comparison with

visual observations. However, human perception is also prone to error, especially for fast movements. The slugs passing by create droplets or a liquid film on the inner side of the glass viewing section, which further hinders observation. Van Hout et al. (2003) stated that even image processing with the help of video cameras is of limited use because the gas–liquid interface is hard to detect for highly aerated slugs. Soedarmo et al. (2019) and Soto-Cortes et al. (2021) proposed objective methods to avoid arbitrary parameter selection in slug detection.

However, besides Zhao et al. (2013), who compared slug frequencies determined with thresholding against those determined by PSD, little attention has been paid to the influence and bias of different calculation methods. Such a comparison is provided in this paper.

To apply different slug frequency calculation methods to the same data set, seven different superficial gas velocities at constant superficial liquid velocity (v_{sl} = 1.87 m/s) and constant diameter (D = 0.097 m) were simulated with OpenFOAM v1812. Four approximations of the liquid level were applied, including h_l^{area}, which is equivalent to evaluating the liquid holdup as often done in experiments. Then, two different approaches were followed to calculate the slug frequency from the liquid level approximations, namely the thresholding and frequency analysis approach. Therefore, a total of eight combinations of liquid level approximation and slug frequency calculation methods were investigated and following observations were made:

1. In the plug flow regime, the plugs show a clear defined shape, the plug liquid holdup is close to one by definition (Yadigaroglu and Hewitt, 2017), and all methods yield similar slug frequencies. Deviations of the slug frequency among the methods are much smaller than in the slug flow regime.
2. The PSD is not sensitive to the method of liquid level determination. However, only the dominant structures are analyzed and, hence, it is not feasible to distinguish between slugs and waves.
3. In the slug flow region, slugs get aerated with increasing superficial gas velocity. Because each method is affected by aeration differently, the methods result in different slug frequencies. Moreover, when approximating the liquid level by h_l^{line} or h_l^{area}, an estimation of the aeration or slug liquid holdup is required, which significantly increases the uncertainty of the prediction.
4. The presented binary methods overcome the problem of adapting the threshold to the degree of aeration. However, they have the disadvantage that droplets in the gas phase might be miscounted as slugs.
5. The proposed h_l^{impr} also accounts for aeration and represents the liquid level better than the other methods. However, it requires detailed knowledge about the liquid volume fraction field data.

Without knowing the exact level of aeration, the height of the waves/slugs cannot be reliably determined from the liquid holdup. Therefore, the methods aiming to directly detect the top of the liquid phase, i.e., h_l^{bin} and h_l^{impr}, performed better in slug detection, especially in distinguishing slugs from waves. Since PSD and liquid holdup both fail to reliably distinguish aerated slugs from waves, methods that can detect whether the liquid structure breaches to the top of the pipe, like h_l^{impr}, are recommended to identify aerated slug structures. Altogether, the paper reveals that the choice of the evaluation method has a significant impact on the resulting slug frequency, especially in the slug flow region. This insight is necessary to judge and compare slug frequencies determined by different research teams utilizing different calculation methods. Furthermore, it helps to choose calculation methods for future research and emphasizes the necessity of standardized slug counting criteria for highly aerated slugs.

To gain further insight into the influence of slug counting criteria on slug frequency, more data with different superficial liquid velocities, diameters, and fluid properties is required. While numerical simulations provide a detailed view of the whole flow field for individual cases, experimental setups are recommended to generate results for a large variety of flow conditions. Furthermore, experiments could validate the behavior of the presented slug detection algorithms for measured data.

CRediT authorship contribution statement

F. Webner: Conceptualization, Methodology, Software, Validation, Formal analysis, Investigation, Visualization, Writing – original draft. **J. Polansky:** Software, Writing – review & editing. **S. Knotek:** Software, Writing – review & editing. **S. Schmelter:** Conceptualization, Methodology, Software, Validation, Formal analysis, Investigation, Writing – original draft, Supervision.

Declaration of competing interest

The authors declare that they have no known competing financial interests or personal relationships that could have appeared to influence the work reported in this paper.

Data availability

Data will be made available on request.

Acknowledgments

This work was supported through the Joint Research Project "Multiphase flow reference metrology". This project has received funding from the EMPIR programme co-financed by the Participating States and from the European Union's Horizon 2020 research and innovation programme.

Appendix A. Review of several slug liquid holdup prediction methods from the literature

In the literature, a variety of different correlations for the prediction of the liquid holdup in slugs can be found. In Pereyra et al. (2012), Ibarra et al. (2019), several of these methods are reviewed. In the following, we briefly introduce a few of these correlations, for which the parameter range is appropriate for the test cases considered in this paper.

Gregory et al. (1978) considered two-phase flow through pipes with internal diameter D = 25.8 mm and D = 51.2 mm. The fluids investigated by them (light oil with a viscosity of $\mu_l = 7 \cdot 10^{-3}$ Pa s and air) had similar fluid properties as the ones considered in this paper. They derive the following correlation for the liquid holdup in slugs:

$$H_{ls}^{\text{Gregory}} = \frac{1}{1 + \left(\frac{v_m}{8.66}\right)^{1.39}}, \tag{A.1}$$

where $v_m = v_{sl} + v_{sg}$ denotes the mixture velocity. In Ibarra et al. (2019), it is stated that even though this correlation is purely based on mixture velocity and does not take into account any other parameters (like pipe diameter or fluid properties), it nevertheless yields reasonable results over a wide range of conditions.

Malnes (1982) evaluated the same data set as Gregory et al. (1978) and proposed a new method by including the influence of gravitation, liquid density, and surface tension into the correlation of Gregory et al. (1978):

$$H_{ls}^{\text{Malnes}} = 1 - \frac{v_m}{83\left(\frac{\sigma g}{\varrho_l}\right)^{0.25} + v_m}, \tag{A.2}$$

where σ is the surface tension, g is the standard gravity, and ϱ_l is the density of the liquid phase.

Ferschneider (1983) evaluated a data set obtained from experiments at 1500 kPa with a natural gas-condensate flow in a large diameter horizontal pipe. Ferschneider developed the following expression for slug liquid holdup:

$$H_{ls}^{\text{Ferschneider}} = \frac{1}{\left[1 + \left(\frac{\hat{\text{Fr}}_m \text{Bo}^{0.1}}{25}\right)^2\right]^2}. \tag{A.3}$$

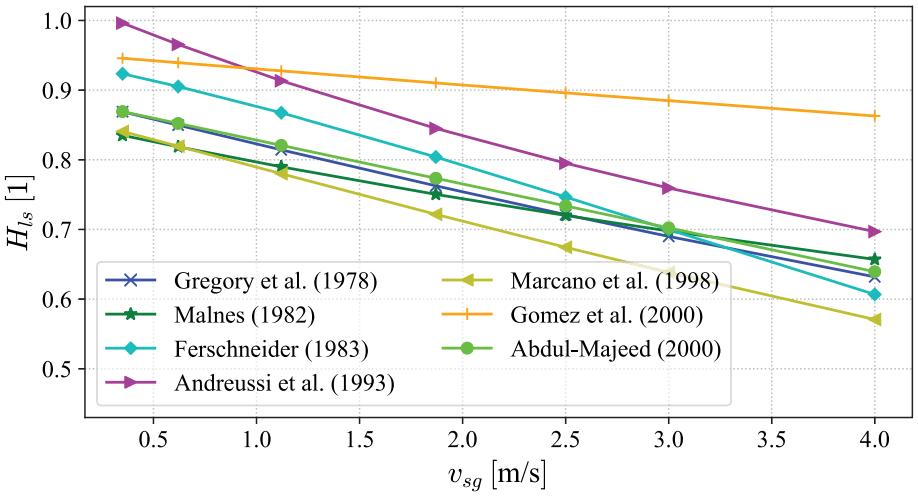

Fig. A.1. Slug liquid holdup correlations from literature. The markers indicate the test cases considered in this paper.

Here $\hat{\mathrm{Fr}}_m$ and Bo denote the mixture Froude number and Bond number, respectively:

$$\hat{\mathrm{Fr}}_m = \frac{v_M}{\sqrt{gD(1-\varrho_l/\varrho_g)}}, \quad \mathrm{Bo} = \frac{(\varrho_l - \varrho_g) g D^2}{\sigma}, \tag{A.4}$$

with density of the gas phase ϱ_g.

Andreussi et al. (1993) investigated air–water flow for three different pipe diameters: $D = 18$ mm, $D = 50$ mm, and $D = 90$ mm. They derived the following correlation, which takes gas and liquid density as well as surface tension into account:

$$H_{ls}^{\text{Andreussi}} = 1 - \frac{\mathrm{Fr}_m - F_0}{\mathrm{Fr}_m + F_1}. \tag{A.5}$$

Here, Fr_m denotes the mixture Froude number, given by

$$\mathrm{Fr}_m = \frac{v_m}{\sqrt{gD}}. \tag{A.6}$$

Furthermore, the coefficients F_0 and F_1 are defined as

$$F_0 = \max\left\{0;\ 2.6\left[1 - 2\left(\frac{0.025}{D}\right)^2\right]\right\}, \quad F_1 = 2400\,\mathrm{Bo}^{-3/4}, \tag{A.7}$$

where Bo denotes the Bond number as given in Eq. (A.4).

Marcano et al. (1998) considered the flow of kerosene ($\mu_l = 1.6 \cdot 10^{-3}$ Pa s) and air through a pipe with inner diameter $D = 77.9$ mm. They propose the following correlation:

$$H_{ls}^{\text{Marcano}} = \frac{1}{1.001 + 0.0587\, v_m + 0.0118\, v_m^2}. \tag{A.8}$$

Gomez et al. (2000) considered a variety of different diameters ($D = 51$ mm, $D = 76$ mm, $D = 178$ mm, and $D = 203$ mm), pipe inclinations (horizontal, inclined, and vertical pipes), liquids (water, kerosene, diesel, and light oil; the latter one within the following range of viscosities: $\mu_l = 1 \ldots 6.5 \cdot 10^{-3}$ Pa s), and gases (air, Freon, and nitrogen). For horizontal pipes, they propose the following correlation:

$$H_{ls}^{\text{Gomez}} = e^{-2.48 \cdot 10^{-6}\,\mathrm{Re}_{slg}}, \tag{A.9}$$

where $\mathrm{Re}_{slg} = \frac{\varrho_l v_m D}{\mu_l}$ denotes the liquid slug Reynolds number.

Abdul-Majeed (2000) also investigated a wide range of different diameters between $D = 25.8$ mm and $D = 203$ mm. His correlation is based on data for several liquids (water, kerosene, diesel, and light oil with viscosity $\mu_l = 1 \ldots 7 \cdot 10^{-3}$ Pa s) and gases (air, Freon, and nitrogen). The correlation takes viscosity into account, but not the density of the fluids. For horizontal pipes, it is given by:

$$H_{ls}^{\text{Abdul-Majeed}} = 1.009 - C_a\, v_m, \quad C_a = 0.006 + 1.3377\,\frac{\mu_g}{\mu_l}. \tag{A.10}$$

Comparison of the slug liquid holdup prediction methods. In Fig. A.1, all the above described slug liquid holdup correlations are plotted for superficial gas velocities between 0 and 7 m/s. All correlations show a decrease of the liquid holdup in slugs for increasing superficial gas velocities. However, the predicted slope of the decrease differs significantly for the different methods. This leads to different predictions of the slug frequency for the test cases considered in this paper depending on which prediction method for the slug liquid holdup is used. Pereyra et al. (2012) fitted the free parameters of these methods to a large, common data set to improve the accuracy. This leads (as expected) to much less spread between the different methods. For the present work, however, the original correlations are employed to illustrate the sensitivity of the slug frequency to slug holdup data that can be found in the literature.

Appendix B. Review of several slug frequency prediction methods from the literature

In the following, several slug frequency prediction methods are reviewed and compared to each other. In Section 5.3, these predictions are also compared with the slug frequencies determined by numerical simulations.

Gregory and Scott (1969) developed one of the earliest slug frequency prediction correlations, and it is still frequently cited. They investigated a carbon dioxide–water flow through pipes of 1.91 cm and 3.51 cm internal diameter at atmospheric pressure and 25 °C. Slugs were counted by measuring pressure pulses and by visual observation. The data points were plotted and a best fit line approach was utilized. The final correlation is given as:

$$f_s^{\text{Greg.–Scott}} = 0.0226\left[\frac{v_{sl}}{gD}\left(\frac{19.75}{v_m} + v_m\right)\right]^{1.2}\ \mathrm{s}^{-1}, \tag{B.1}$$

where v_m is the mixture velocity. It should be noted that units are commonly omitted in slug frequency formulas. For example in Eq. (B.1), 19.75 $\frac{\mathrm{m}^2}{\mathrm{s}^2}$ instead of 19.75 would be physically correct.

Heywood and Richardson (1979) applied the method by Gregory and Scott (1969) and tuned it on their experimental data of a 4.2 cm internal diameter pipe. They determined the slug frequency by the means of a PSD analysis. The resulting correlation is:

$$f_s^{\text{Heyw.–Rich.}} = 0.0434\left[\frac{v_{sl}}{v_m}\left(\frac{2.02}{D} + \frac{v_m^2}{gD}\right)\right]^{1.02}\ \mathrm{s}^{-1}. \tag{B.2}$$

Jepson and Taylor (1993) studied general flow characteristics and flow patterns of a large diameter pipe with 30 cm internal diameter. They combined their data with experimental data of Nicholson et al.

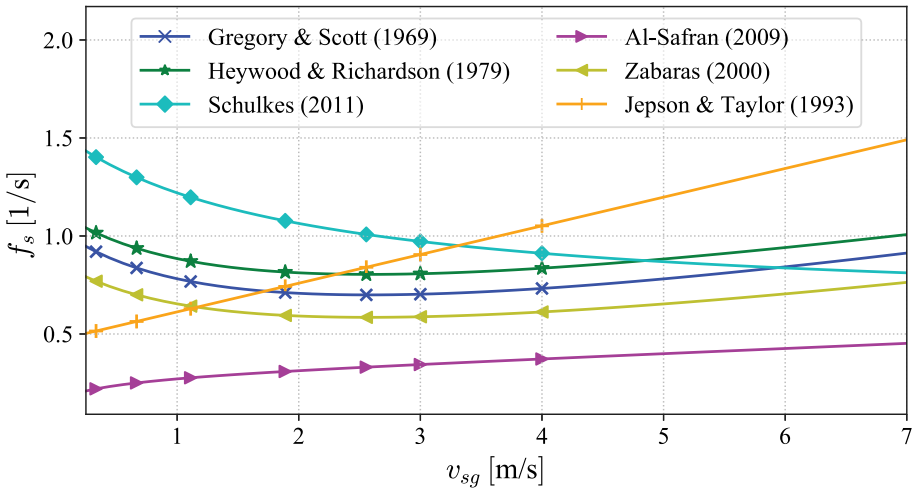

Fig. B.1. Slug frequency predictions from literature. The markers indicate the test cases considered in this paper.

(1978), who investigated 2.54 cm and 5.12 cm internal diameter pipes. Jepson and Taylor (1993) found the following correlation:

$$f_s^{\text{Jeps.–Tayl.}} = \frac{v_{sl}}{D}\left(7.59\times10^{-3}v_m + 0.01\right)\text{s}^{-1}. \tag{B.3}$$

Zabaras (2000) compared existing slug frequency prediction methods to a data set of 399 data points. 194 of those data points were collected from published literature that covered internal diameters ranging from 2.54 cm to 20.32 cm. Slug frequency data of various fluid properties were included in the data set and the inclination angle was varied between 0° and 11°. Zabaras (2000) adapted the approach from Gregory and Scott (1969) to the collected data and found the following correlation:

$$f_s^{\text{Zabaras}} = 0.0226\left[\frac{v_{sl}}{gD}\left(\frac{19.75}{v_m}+v_m\right)\right]^{1.2}\left(0.836+2.75\sin^{0.25}(\gamma)\right)\text{s}^{-1}, \tag{B.4}$$

where γ is the inclination angle. For an inclination of 0°, as discussed in this paper, Eq. (B.4) yields:

$$f_s^{\text{Zabaras}} = 0.0189\left[\frac{v_{sl}}{gD}\left(\frac{19.75}{v_m}+v_m\right)\right]^{1.2}\text{s}^{-1}. \tag{B.5}$$

Al-Safran (2009) analyzed 230 data points published in literature (where the internal diameters ranged between 2.5 cm and 20.3 cm) to develop a new slug frequency prediction method:

$$f_s^{Al-Safran} = v_l^{1.53}\exp(0.8+0.27\left(\frac{v_g-v_l}{v_m}\right)-34.1\,D)\ \text{s}^{-1}, \tag{B.6}$$

where v_l and v_g are the actual liquid velocity and gas velocity, respectively. To calculate the actual velocities of the fluids, the occupied cross section of each phase is required. The procedure by Taitel and Dukler (1976) is utilized to calculate the liquid level and the gas and liquid velocity.

Schulkes (2011) investigated the influence of several parameters on slug frequency. Published data with a total of about 1200 data points were used. He found that fluid properties like density and viscosity can be neglected for turbulent flow, but should be considered for laminar flow. Furthermore, he found no significant correlation between pressure and slug frequency. Schulkes (2011) developed a new correlation based on the collected data:

$$f_s^{\text{Schulkes}} = 0.016\,\frac{v_{sl}}{D}\left(2+3\frac{v_{sl}}{v_m}\right). \tag{B.7}$$

Eq. (B.7) is for horizontal and turbulent flow. For laminar flow, typically fluids with high viscosity, and/or inclined pipes, correction factors can be applied.

Comparison of the slug frequency prediction methods. Fig. B.1 shows the described slug frequency prediction methods from literature for horizontal flow at a superficial liquid velocity of 1.87 m/s and an internal diameter of 0.097 m. The slug frequency f_s is plotted against superficial gas velocity v_{sg}. The markers refer to the flow conditions considered in this paper.

Even though one would expect an equal or similar slug frequency at same flow conditions, a large range of slug frequencies is covered by the different prediction methods. Several different trends can be observed: The methods by Jepson and Taylor (1993) and Al-Safran (2009) exhibit a monotonically increasing trend, whereas the curve by Schulkes (2011) decreases monotonically. The prediction methods by Heywood and Richardson (1979) and Zabaras (2000) are inspired by Gregory and Scott (1969). Hence, these three methods show a similar trend, with a local minimum between 2 m/s and 3 m/s. Further analyses, differences and similarities of different slug frequency prediction methods from the literature can be found in Webner (2021).

References

Abdul-Majeed, G., 2000. Liquid slug holdup in horizontal and slightly inclined two-phase slug flow. J. Pet. Sci. Eng. 27, 27–32.
Al-Safran, E.M., 2009. Investigation and prediction of slug frequency in gas/liquid horizontal pipe flow. J. Pet. Sci. Eng. 69, 143–155.
Andreussi, P., Minervini, A., Paglianti, A., 1993. Mechanistic model of slug flow in near-horizontal pipes. AIChE J. 39, 1281–1291.
Andritsos, N., Hanratty, T.J., 1987. Influence of interfacial waves in stratified gas-liquid flows. AIChE J. 33 (3), 444–454.
Baba, Y.D., Archibong, A.E., Aliyu, A.M., Ameen, A.I., 2017. Slug frequency in high viscosity oil-gas two-phase flow: Experiment and prediction. Flow Meas. Instrum. 54, 109–123.
Dukler, A.E., Hubbard, M.G., 1975. A model for gas-liquid slug flow in horizontal and near horizontal tubes. Ind. Eng. Chem. Fundam. 14 (4), 337–347.
El-Oun, Z., 1990. Gas-liquid two-phase flow in pipelines. In: SPE Annual Technical Conference and Exhibition. OnePetro.
Fabre, J., Liné, A., Gadoin, E., 1995. Void and pressure waves in slug flow. In: IUTAM Symposium on Waves in Liquid/Gas and Liquid/Vapour Two-Phase Systems. Springer, pp. 25–44.
Ferschneider, G., 1983. Ecoulements diphasiques gaz-liquide à poches et à bouchons en conduites. Revue de l'Institut Français du Pétrole 38 (2), 153–182.
Gokcal, B., Al-Sarkhi, A.S., Sarica, C., Al-Safran, E.M., 2009. Prediction of slug frequency for high-viscosity oils in horizontal pipes. In: SPE Annual Technical Conference and Exhibition. Society of Petroleum Engineers, New Orleans, Louisiana.
Gomez, L., Shoham, O., Taitel, Y., 2000. Prediction of slug liquid holdup: horizontal to upward vertical flow. Int. J. Multiph. Flow. 26, 517–521.
Gregory, G.A., Nicholson, M., Aziz, K., 1978. Correlation of the liquid volume fraction in the slug for horizontal gas-liquid slug flow. Int. J. Multiph. Flow. 4, 33–39.
Gregory, G.A., Scott, D.S., 1969. Correlation of liquid slug velocity and frequency in horizontal cocurrent gas-liquid slug flow. AIChE J. 15, 933–935.
Hernandez-Perez, V., Abdulkadir, M., Azzopardi, B.J., 2010. Slugging frequency correlation for inclined gas-liquid flow. Int. J. Chem. Molecular Eng. 4 (1), 10–17.

Heywood, N., Richardson, J.F., 1979. Slug flow of air-water mixtures in a horizontal pipe: Determination of liquid holdup by γ-ray absorption. Chem. Eng. Sci. 34, 17–30.

Hill, T., Wood, D., 1990. A new approach to the prediction of slug frequency. In: SPE Annual Technical Conference and Exhibition. SPE.

Hill, T., Wood, D., 1994. Slug flow: Occurrence, consequences, and prediction. In: University of Tulsa Centennial Petroleum Engineering Symposium. Society of Petroleum Engineers.

Hirt, C.W., Nichols, B.D., 1981. Volume of fluid /VOF/ method for the dynamics of free boundaries. J. Comput. Phys. 39, 201–225.

Ibarra, R., Nossen, J., Tutkun, M., 2019. Holdup and frequency characteristics of slug flow in concentric and fully eccentric annuli pipes. J. Pet. Sci. Eng. 182, 106256.

Jepson, W.P., Taylor, R.E., 1993. Slug flow and its transitions in large-diameter horizontal pipes. Int. J. Multiph. Flow. 19, 411–420.

Knotek, S., Fiebach, A., Schmelter, S., 2016. Numerical simulation of multiphase flows in large horizontal pipes. In: 17th International Flow Measurement Conference. FLOMEKO, Sydney, Australia.

Knotek, S., Schmelter, S., Olbrich, M., 2021. Assessment of different parameters used in mesh independence studies in two-phase slug flow simulations. Measur.: Sensors 18, 100317.

Malnes, D., 1982. Slug flow in vertical, horizontal and inclined pipes. Technical Report IFE/KR/E-83/002, V. Inst. for Energy technology, Kjeller, Norway.

Mandhane, J., Gregory, G., Aziz, K., 1974. A flow pattern map for gas-liquid flow in horizontal pipes. Int. J. Multiph. Flow. 1, 537–553.

Marcano, R., Chen, X., Sarica, C., Brill, J., 1998. A study of slug characteristics for two-phase horizontal flow. In: SPE International Oil Conference and Exhibition in Mexico. SPE, SPE-39856-MS.

Menter, F.R., 1993. Two-equation eddy-viscosity turbulence models for engineering applications. AIAA J. 32, 1598–1605.

Nicholson, M.K., Aziz, K., Gregory, G.A., 1978. Intermittent two phase flow in horizontal pipes: Predictive models. Can. J. Chem. Eng. 56 (6), 653–663.

Nydal, O.J., 1991. An Experimental Investigation on Slug Flow (Ph.D. thesis). University of Oslo, Department of Mathematics.

Olbrich, M., Bär, M., Oberleithner, K., Schmelter, S., 2021a. Statistical characterization of horizontal slug flow using snapshot proper orthognal decomposition. Int. J. Multiph. Flow. 134, 103453.

Olbrich, M., Hunt, A., Leonard, T., van Putten, D.S., Bär, M., Oberleithner, K., Schmelter, S., 2021b. Comparing temporal characteristics of slug flow from tomography measurements and video observations. Measur.: Sensors 18, 100222.

Pereyra, E., Arismendi, R., Gomez, L.E., Mohan, R.S., Shoham, O., Kouba, G.E., 2012. State of the art of experimental studies and predictive methods for slug liquid holdup. J. Energy Resour. Technol. 134 (2).

Pineda-Pérez, H., Kim, T., Pereya, E., Ratkovich, R., 2018. CFD modeling of air and highly viscous liquid two-phase slug flow in horizontal pipes. Chem. Eng. Res. Des. 136, 638–653.

Schmelter, S., Knotek, S., Olbrich, M., Fiebach, A., Bär, M., 2021a. On the influence of inlet perturbations on slug dynamics in horizontal multiphase flow – a computational study. Metrologia 58, 014003.

Schmelter, S., Olbrich, M., Knotek, S., Bär, M., 2021b. Analysis of multiphase flow simulations and comparison with high-speed video observations. Measur.: Sensors 18, 100154.

Schmelter, S., Olbrich, M., Schmeyer, E., Bär, M., 2020. Numerical simulation, validation, and analysis of two-phase slug flow in large horizontal pipes. Flow Meas. Instrum. 73, 101722.

Schulkes, R., 2011. Slug frequencies revisited. In: 15th International Conference on Multiphase Production Technology. Cannes, France.

Soedarmo, A.A., Rodrigues, H.T., Pereyra, E., Sarica, C., 2019. A new objective and distribution-based method to characterize pseudo-slug flow from wire-mesh-sensors (WMS) data. Exp. Therm Fluid Sci. 109, 109855.

Soto-Cortes, G., Pereyra, E., Sarica, C., Torres, C., Soedarmo, A., 2021. Signal processing for slug flow analysis via a voltage or instantaneous liquid holdup time-series. Flow Meas. Instrum. 79, 101968.

Taitel, Y., Dukler, A.E., 1976. A model for predicting flow regime transitions in horizontal and near horizontal gas-liquid flow. AIChE J. 22, 47–55.

The MathWorks, Inc., 2019. Signal processing toolbox reference. Revised for Version 8.2 (Release 2019a).

Van Hout, R., Shemer, L., Barnea, D., 2003. Evolution of hydrodynamic and statistical parameters of gas–liquid slug flow along inclined pipes. Chem. Eng. Sci. 58 (1), 115–133.

Webner, F., 2021. Numerical Simulation of Slug Flow in Horizontal Pipes and Comparison with Slug Frequency Prediction Methods from Literature. (Master's thesis). Technical University Berlin, Germany.

Woods, B.D., Fan, Z., Hanratty, T.J., 2006. Frequency and development of slugs in a horizontal pipe at large liquid flows. Int. J. Multiph. Flow. 32 (8), 902–925.

Woods, B.D., Hanratty, T.J., 1999. Influence of froude number on physical processes determining frequency of slugging in horizontal gas–liquid flows. Int. J. Multiph. Flow. 25 (6–7), 1195–1223.

Yadigaroglu, G., Hewitt, G.F., 2017. Introduction to Multiphase Flow: Basic Concepts, Applications and Modelling. Springer.

Zabaras, G., 2000. Prediction of Slug Frequency for Gas/Liquid Flows. SPE J. 5 (03), 252–258.

Zhao, Y., Yeung, H., Lao, L., 2013. Slug frequency in high viscosity liquid and gas flow in horizontal pipes. In: 16th International Conference on Multiphase Production Technology.